

Cone Photoreceptor Dysfunction in Early-Stage Diabetic Retinopathy: Association Between the Activation Phase of Cone Phototransduction and the Flicker Electroretinogram

J. Jason McAnany^{1,2} and Jason C. Park¹

¹Department of Ophthalmology and Visual Sciences, University of Illinois at Chicago, Chicago, Illinois, United States

²Department of Bioengineering, University of Illinois at Chicago, Chicago, Illinois, United States

Correspondence: J. Jason McAnany, Department of Ophthalmology and Visual Sciences, University of Illinois at Chicago, 1855 West Taylor Street, MC/648, Chicago, IL 60612, USA; jmcana1@uic.edu.

Submitted: October 9, 2018
Accepted: November 21, 2018

Citation: McAnany JJ, Park JC. Cone photoreceptor dysfunction in early-stage diabetic retinopathy: association between the activation phase of cone phototransduction and the flicker electroretinogram. *Invest Ophthalmol Vis Sci.* 2019;60:64–72. <https://doi.org/10.1167/iovs.18-25946>

PURPOSE. To define the nature and extent of cone photoreceptor abnormalities in diabetic individuals who have mild or no retinopathy by assessing the activation phase of cone phototransduction and the flicker ERG in these individuals.

METHODS. Light-adapted single-flash and flicker ERGs were recorded from 20 diabetic individuals who have no clinically apparent retinopathy (NDR), 20 diabetic individuals who have mild nonproliferative diabetic retinopathy (NPDR), and 20 nondiabetic, age-equivalent controls. A-waves elicited by flashes of different retinal illuminance were fit with a delayed Gaussian model to derive R_{mp3} (maximum amplitude of the massed photoreceptor response) and S (phototransduction sensitivity). Fundamental amplitude and phase of ERGs elicited by full-field sinusoidal flicker were obtained across a frequency range of 6 to 100 Hz.

RESULTS. ANOVA indicated that both diabetic groups had significant S losses compared with the controls, whereas mean R_{mp3} did not differ significantly among the groups. ANOVA also indicated significantly reduced flicker ERG amplitude for frequencies ≥ 56 Hz for both diabetic groups compared with the controls. Flicker ERG timing (phase) did not differ significantly among the groups. $\log R_{mp3} + \log S$ was significantly correlated with the patients' high-frequency (62.5 Hz) flicker ERG amplitude loss ($r = 0.69$, $P < 0.001$).

CONCLUSIONS. The delayed Gaussian a-wave model is useful for characterizing abnormalities in the activation phase of cone phototransduction and can help explain flicker ERG abnormalities in early-stage diabetic retinopathy. Reduced cone sensitivity and attenuated high-frequency flicker ERGs provide evidence for impaired cone function in these individuals.

Keywords: electroretinogram, diabetic retinopathy, photoreceptors, a-wave, flicker electroretinogram

Diabetic retinopathy (DR) has traditionally been considered a complication of diabetes mellitus (DM) that manifests as a retinal vasculopathy. More recently, however, there has been wider recognition of diabetic retinal neurodegeneration that can accompany, or precede, the clinically apparent vascular changes.^{1–5} Studies of diabetic retinal neurodegeneration have focused primarily on abnormalities of inner-retina structure and function. These studies have reported reduced retinal ganglion cell layer thickness assessed by optical coherence tomography,^{6–9} as well as functional abnormalities of the pattern ERG,^{10–14} photopic negative response of the single-flash ERG,^{15,16} scotopic threshold response,¹⁷ and the melanopsin-mediated pupillary light reflex,^{18,19} all of which are generated primarily by retinal ganglion cells. In addition, there have been reports of abnormalities of the oscillatory potentials (OPs) in early-stage DR, which are generated, at least in part, by inner-retina neurons (see Tzekov and Arden²⁰ for a review). The OPs are a series of high-frequency wavelets that are superimposed on the ascending limb of the b-wave and are sensitive to disturbances in retinal circulation.²⁰

Despite the focus on inner-retina neurodegeneration, there is mounting evidence suggesting a fundamental role of the photoreceptors in the pathology of the disease.^{21–24} For example, in an electrophysiological study of photoreceptor function in diabetic individuals, Holopigian et al.²² reported light- and dark-adapted ERG deficits that were consistent with photoreceptor sensitivity loss. That study²² derived the activation phase of rod and cone phototransduction from the leading edge of the a-wave using the delayed Gaussian model of Hood and Birch.^{25,26} From this model, two primary parameters were obtained: R_{mp3} , the maximum amplitude of the massed photoreceptor response (Granit's P3 response), and S , which is related to the sensitivity of the activation phase of phototransduction. Holopigian et al.²² found S reductions in 9 of their 12 diabetic subjects who had a wide range of retinopathy severity; only two of their diabetic subjects had reduced R_{mp3} .

More recently, our group reported a selective high-frequency amplitude attenuation of the flicker ERG in diabetic individuals who had no clinically apparent retinopathy (NDR), as well as in diabetic individuals who had mild nonproliferative DR (mild NPDR).^{27,28} The temporal frequency

deficits in the flicker ERG were interpreted within a cascade model of retinal processing^{29,30} that suggested that the site of the abnormal temporal filtering is likely at the photoreceptors, consistent with the photoreceptor dysfunction measured by Holopigian et al.²²

Although modeling the leading edge of the cone a-wave and recording the flicker ERG appear to be disparate approaches to studying cone pathway dysfunction in DR, previous work has shown that these measures are, in fact, related.³¹ The rationale linking the phototransduction parameters of the cone a-wave and the flicker ERG is discussed in detail elsewhere.³¹ In brief, R_{mp3} corresponds to the maximum amplitude of the massed photoreceptor response and the value of R_{mp3} would be reduced, for example, by a loss of cone photoreceptors, assuming that the remaining cones respond normally.³² In terms of the flicker ERG, an R_{mp3} reduction is expected to reduce the flicker ERG amplitude proportionally across all temporal frequencies. A reduction in S corresponds to a cone photoreceptor sensitivity loss, and is equivalent to viewing the stimulus through a neutral density filter (e.g., dark glasses). Reductions in S could be due, for example, to abnormalities within the phototransduction cascade.^{25,33} Consequently, S loss attenuates the stimulus mean luminance and the peak luminance equally, leaving the stimulus contrast unaltered. The predictions for the effect of an S reduction on the flicker ERG depend on the temporal frequency of the flicker stimulus. That is, for low to moderate temporal frequencies, the flicker ERG is characterized by Weber-law adaptation, such that response amplitude is largely dependent on stimulus contrast and minimally dependent on mean luminance.³⁴ For moderate to high temporal frequencies, Weber-law adaptation is less apparent and response amplitude depends on mean luminance.³⁴ Consequently, S loss is expected to reduce the high-frequency flicker ERG amplitude (above approximately 40 Hz) more than the low-frequency flicker ERG amplitude.³¹ This expected relationship between log S and flicker ERG amplitude has been established in patients who have retinitis pigmentosa.³¹

The goal of the present study was to gain a more complete understanding of the nature and extent of cone photoreceptor abnormalities in diabetic individuals who have NDR or mild NPDR. Specifically, we sought to determine if abnormalities in the activation phase of cone phototransduction have predictable effects on the flicker ERG in early-stage DR. This finding would help to link the seemingly unrelated reports of reduced cone a-wave sensitivity²² and high-frequency flicker ERG attenuation^{27,28} in these individuals. Furthermore, support for abnormalities in the activation phase of cone phototransduction and high-frequency flicker ERG attenuation would add to growing evidence that implicates a role for cone photoreceptor dysfunction in early-stage DR.

METHODS

Subjects

This research project followed the tenets of the Declaration of Helsinki and was approved by an institutional review board at the University of Illinois at Chicago. All subjects provided written informed consent before participating. Forty individuals diagnosed with type-2 DM were recruited from the Department of Ophthalmology and Visual Sciences at the University of Illinois at Chicago. Comprehensive histories were obtained from their medical records and each subject was examined by a retina specialist. The stage of NPDR was graded and the subjects were clinically classified as diabetic with no clinically apparent DR ($n = 20$) or diabetic with mild NPDR (n

TABLE. Subject Characteristics

	Control, <i>N</i> = 20	NDR, <i>N</i> = 20	Mild NPDR, <i>N</i> = 20
Age, y	51.9 ± 12.2	52.0 ± 8.2	53.7 ± 8.6
Sex	8M 12F	5M 15F	8M 12F
Log MAR acuity	-0.05 ± 0.06	-0.01 ± 0.06	-0.01 ± 0.06
Disease duration, y		7.8 ± 5.5	16.0 ± 8.4
HbA1c (%)		7.9 ± 1.9	8.4 ± 1.6

y, years; M, male; F, female; MAR, minimum angle of resolution; HbA1c, glycated hemoglobin.

= 20) according to the early treatment of DR study (ETDRS) scale.³⁵ Subjects classified as mild NPDR had retinal vascular abnormalities, including microaneurysms, hard exudates, cotton-wool spots, and/or mild retinal hemorrhage (equivalent to ETDRS level 35 or less³⁵). Other than diabetes, no subject had systemic disease known to affect retinal function or ocular disease. Individuals who had sickle cell disease, retinal vascular occlusions, AMD, glaucoma, or high myopia were not recruited. The lens of each subject was graded by slit lamp examination using a subjective clinical scale that ranged from clear to 4+. Subjects with nuclear sclerotic, posterior subcapsular, or cortical lens opacities greater than 2+ were excluded. Subject characteristics, including age, sex, visual acuity, estimated diabetes duration, and HbA1c percentage, are provided in the Table. With the exception of three mild NPDR subjects who had a history of anti-VEGF injection, no subject had received treatment for DR.

Twenty visually normal, nondiabetic, control subjects also participated. All control subjects had best-corrected visual acuity of 0.06 logMAR (equivalent to approximately 20/23 Snellen acuity) or better, as assessed with the Lighthouse distance visual acuity chart, and normal letter contrast sensitivity as measured with a Pelli-Robson chart. The mean age of the control subjects did not differ significantly from that of the diabetic subjects ($F = 0.21$, $P = 0.81$). Of note, 15 of the control subjects and 36 of the diabetic subjects participated in a previous study of ERG abnormalities in early-stage DR.²⁸

Apparatus, Stimuli, and Procedure

Single-flash and flicker stimuli were generated by and presented in a ColorDome desktop Ganzfeld system (Diagnosys LLC, Lowell, MA, USA) that we have used previously and described elsewhere.^{27,36} The spectral characteristics of the stimuli were calibrated with a PR-740 SpectraScan spectroradiometer (Photo Research/JADAK, Inc; Syracuse, NY, USA) and luminance values were calculated based on $V_{10\lambda}$. Measurements from all subjects were performed monocularly, with the fellow eye patched. For the DM subjects, the stage of NPDR was generally the same for the two eyes. For rare cases in which the disease stage differed between eyes, the eye with the lower NPDR stage was tested. The pupil of the tested eye was dilated with 2.5% phenylephrine hydrochloride and 1% tropicamide drops. ERGs were recorded with DTL electrodes, and gold-cup electrodes were used as reference (ear) and ground (forehead). Amplifier bandpass settings were 0.30 to 500 Hz and the sampling frequency was 2 kHz.

The flicker ERG was recorded across a broad range of stimulus temporal frequencies, based on a paradigm that is described in detail elsewhere.²⁸ In brief, the subject was first light-adapted for 2 minutes to a uniform field that was composed of 3.7 log Td of middle-wavelength light (516-nm peak) and 3.7 log Td long-wavelength light (632-nm peak), assuming a dilated pupil diameter of 8 mm. The uniform field was modulated sinusoidally at temporal frequencies ranging

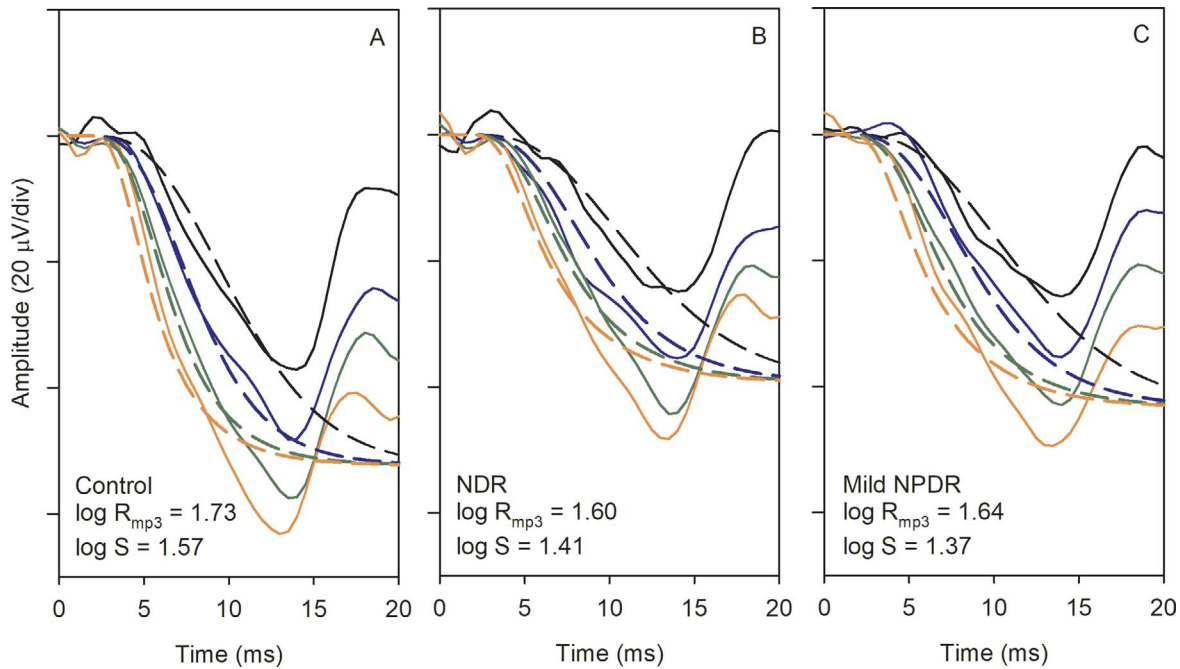


FIGURE 1. Mean single-flash ERG waveforms recorded for a series of flash retinal illuminances (2.8 log Td-s, black; 3.2 log Td-s, blue; 3.6 log Td-s, green; 4.0 log Td-s, orange). The dashed lines represent the delayed Gaussian model fit to the traces of the corresponding color. Data are shown for the controls (A), NDR subjects (B), and mild NPDR subjects (C). The $\log R_{mp3}$ and $\log S$ parameters for the fits to the mean data are given.

from 6.3 to 100 Hz in steps of approximately 0.06 log units. The Michelson contrast of the sinusoidal modulation was 100%. Each flicker train had a duration of approximately 1 second, with the exact duration depending on the stimulus period. A minimum of five responses for each temporal frequency were obtained and averaged for analysis. Between presentations of the flicker stimulus, the ganzfeld was illuminated uniformly by the steady adapting field.

Following the flicker ERG recordings, the activation phase of cone phototransduction was assessed using a paradigm developed in previous studies.^{31,32} Specifically, full-field ERGs were elicited by brief (<1 ms) achromatic flashes of 2.8, 3.2, 3.6, and 4.0 log Td-s (assuming a dilated pupil diameter of 8 mm) that were generated by the xenon strobe of the ColorDome. The xenon flashes were presented against an LED-generated achromatic adapting field of 3.3 log Td. A minimum of five responses for each flash retinal illuminance were obtained and averaged for analysis.

Analysis

The initial and final few cycles of the flicker waveforms were omitted, as these cycles can contain onset and offset transients. Spectral analysis of the remaining steady-state response was performed to derive the amplitude and phase of the flicker ERG. In figures 4 and 5, the amplitudes represent the full trough-to-peak amplitude of the fundamental and the phase measures were “unwrapped” to extend beyond 360°.

The leading edges of the a-waves elicited by the four flash retinal illuminances were ensemble-fit using the delayed Gaussian model of Hood and Birch.²⁶ This model describes the massed photoreceptor response of the cone system to a brief flash of retinal illuminance (I) as a function of time (t) as follows:

$$P3(I, t) = R_{mp3} \{1 - \exp[-IS(t - t_d)^2]\} \otimes \exp[-(t/\tau)], \quad (1)$$

where R_{mp3} is the maximum amplitude of P3 response, S represents the sensitivity of phototransduction, t_d defines the

delay before the onset of the response, \otimes represents convolution, and τ defines the time constant of a low-pass exponential filter due to cone outer segment capacitance. For consistency with previous work, the value of t_d was fixed at 2 ms and τ was 1.8.³¹

RESULTS

Cone Phototransduction Parameters

Figure 1 shows the mean single-flash a-waves for the control subjects (A), NDR subjects (B), and mild NPDR subjects (C). To permit visualizing the a-waves, only the first 20 ms of the ERGs are shown. The solid lines represent the mean amplitude of the response elicited by stimuli of different retinal illuminance and the dashed lines represent the fits of the Hood and Birch model²⁶ (Equation 1) to the a-waves. The model provided a good description of the waveforms, but the a-wave amplitudes tended to be larger than the derived P3 component at the higher flash intensities, consistent with previous work,^{31,32} likely due to postreceptor contributions to the a-wave.^{37–40} As indicated by the parameter values shown in Figure 1, the control subjects had both larger $\log R_{mp3}$ and $\log S$ values, on average, as compared with the NDR and mild NPDR subjects.

The $\log R_{mp3}$ and $\log S$ values were obtained for each subject and are plotted in Figure 2. The vertical and horizontal dashed lines mark the lower limit of the control range of $\log S$ and $\log R_{mp3}$, respectively. Subjects with reduced $\log S$ have data points that fall to the left of the vertical line, whereas subjects with reduced $\log R_{mp3}$ have data points that fall below the horizontal line. It is clear that many NDR and mild NPDR subjects had reduced $\log S$ (60% of the NDR and 40% of the mild NPDR). Reductions in $\log R_{mp3}$ were less common (20% of the NDR and 20% of the mild NPDR). Only three DM subjects had reductions in both $\log S$ and $\log R_{mp3}$. One-way ANOVAs were performed to compare the $\log R_{mp3}$ and $\log S$ parameters among the three groups. For the $\log R_{mp3}$

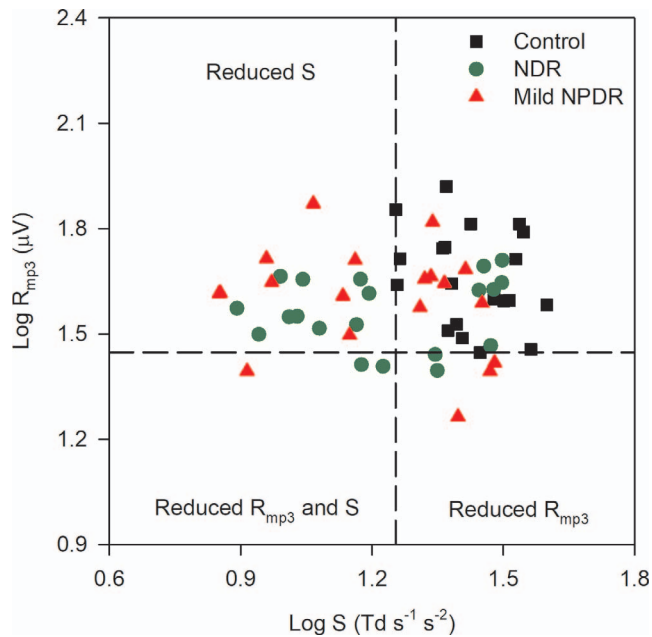


FIGURE 2. $\log R_{mp3}$ is plotted as a function of $\log S$ for the controls (black squares), NDR subjects (green circles), and mild NPDR subjects (red triangles). The vertical dashed line marks the lower limit of the control $\log S$ and the horizontal dashed line marks the lower limit of the control $\log R_{mp3}$.

parameter, there was a nonsignificant trend for differences among the three groups (control, NDR, mild NPDR; $F = 2.85$, $P = 0.07$). In contrast, the $\log S$ parameter did differ significantly among the three groups ($F = 9.49$, $P < 0.001$). Holm-Sidak pairwise comparisons indicated a statistically significant reduction in $\log S$ for the NDR ($t = 3.61$, $P = 0.001$) and mild NPDR ($t = 3.92$, $P < 0.001$) groups compared with the control group. However, the NDR and mild NPDR $\log S$ values did not

differ significantly ($t = 0.31$, $P = 0.76$). Thus, both patient groups had statistically significant $\log S$ reductions compared with the controls, but $\log R_{mp3}$ was statistically equivalent among the groups.

Flicker ERG Amplitude and Phase Across Temporal Frequency

Figure 3 shows the mean flicker ERG traces recorded at 31.25 Hz (A) and 62.5 Hz (B) for the controls (black), NDR subjects (green), and mild NPDR subjects (red). For clarity, only four response cycles obtained near the middle of the flicker train are shown. The general shape and timing of the waveforms were highly similar for the three groups. However, there was a clear amplitude reduction for the NDR and mild NPDR groups for the 62.5-Hz response that was less apparent at 31.25 Hz.

Figure 4 shows the mean (\pm SEM) \log fundamental amplitude (A) and phase (B) as a function of \log temporal frequency for the controls (black), NDR subjects (green), and mild NPDR subjects (red). The solid gray line represents the noise level, defined as the mean amplitude of the frequencies that neighbor the stimulus frequency (approximately 1.5 Hz above and below each stimulus frequency). The mean amplitude for each subject group was above the noise level at all temporal frequencies, but for some individual DM subjects, amplitudes at high temporal frequencies had low signal-to-noise ratios (SNRs). There were small differences among the three groups for the four lowest temporal frequencies examined (6 Hz to 12.5 Hz); however, these differences may not be reliable, as recordings had substantial low-frequency noise contamination (as indicated by the gray line). The amplitudes for the three groups were highly similar for frequencies between approximately 16 Hz and 27 Hz. For higher temporal frequencies, systematic differences among the groups become apparent, with control subjects having larger amplitude responses than the DM subjects. In contrast, the phase of the fundamental response (Fig. 4B) was highly similar for the three groups at all temporal frequencies.

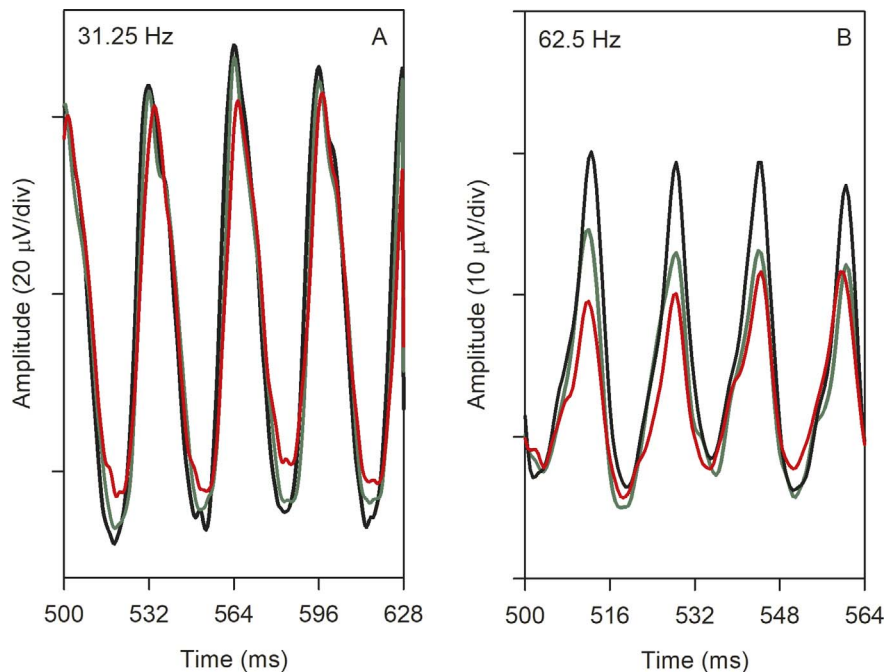


FIGURE 3. Mean ERG waveforms recorded at 31.25 Hz (A) and 62.5 Hz (B) for the control subjects (black), NDR subjects (green), and mild NPDR subjects (red). For clarity, only four cycles that were recorded near the middle of the flicker train are shown.

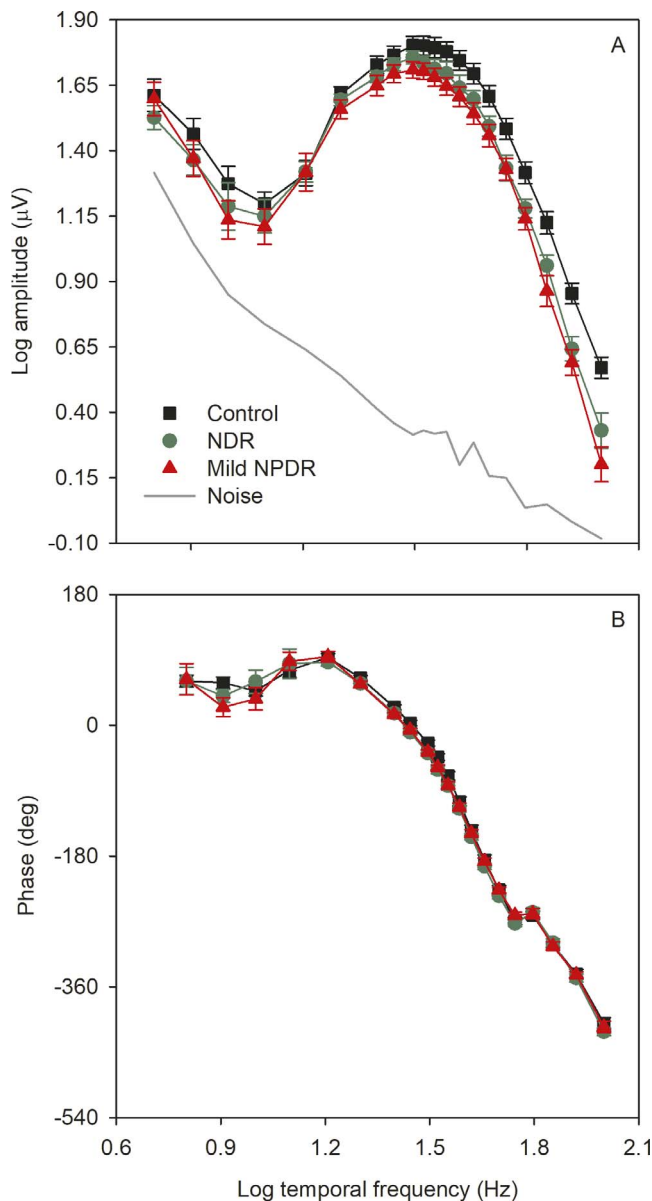


FIGURE 4. Mean (\pm SEM) log fundamental amplitude (A) and phase (B) as a function of log stimulus temporal frequency. Control subjects are shown in black (squares), NDR subjects are shown in green (circles), mild NPDR subjects are shown in red (triangles).

A repeated-measures 2-way ANOVA, with main effects of group (control, NDR, mild NPDR) and stimulus frequency, was performed to compare the log amplitudes among the groups. There were significant effects of group ($F = 4.56$, $P = 0.015$) and stimulus frequency ($F = 364.00$, $P < 0.001$), as well as a significant interaction between these main effects ($F = 1.84$, $P = 0.002$). Holm-Sidak pairwise comparisons indicated a statistically significant reduction in mean amplitude for the mild NPDR group for frequencies of 45.5 Hz and greater (all $t > 2.30$, $P < 0.05$). For the NDR group, pairwise comparisons indicated a statistically significant reduction in mean amplitude for frequencies of 55.6 Hz and greater (all $t > 2.09$, $P < 0.04$).

A repeated-measures 2-way ANOVA, with main effects of group (control, NDR, mild NPDR) and stimulus frequency was performed to compare the phases among the groups. There was no significant effect of group ($F = 1.34$, $P = 0.27$), but there was a significant effect of stimulus frequency ($F =$

1359.90, $P < 0.001$). The interaction between these effects was not significant ($F = 0.68$, $P = 0.93$). Thus, there were no significant phase differences among the subject groups.

Relationship Between the Cone Phototransduction and Flicker ERG Measures

Previous work has shown that a reduction in R_{mp3} results in decreased flicker ERG amplitude across all temporal frequencies.³¹ The decrease is expected to be proportional across temporal frequency, which would produce a uniform downward shift of the control flicker function shown in Figure 4A. By contrast, the effect of reduced S on the flicker ERG amplitude is more complex, exhibiting a temporal frequency dependence.³¹ As discussed in the introductory section, a reduction in S is expected to attenuate the amplitude of the flicker ERG at high temporal frequencies, with relatively little effect on the amplitude elicited by slow flicker. These predictions are evaluated in Figure 5 by comparing flicker ERG amplitude (31.25 Hz, top row; 62.5 Hz, bottom row) and the derived a-wave parameters (log R_{mp3} , first column; log S , second column; log $R_{mp3} + S$, third column). The data in these panels have been normalized to the control mean to facilitate comparisons across the two frequencies and a-wave parameter type. For example, in Figure 5A, a value of -0.6 indicates a 0.6 log unit loss of the 31.25 Hz flicker ERG amplitude (y -axis) and a 0.6 log unit loss of R_{mp3} (x -axis), relative to the control mean. The dashed line is the equality line that indicates equal losses for both parameters plotted. Data are shown for the 31.25-Hz flicker stimulus because this is near the middle of the flicker range that was examined; this is also the International Society for Clinical Electrophysiology of Vision (ISCEV) standard flicker frequency. Data are shown at 62.5 Hz because this was the highest temporal frequency for which every subject had a flicker response that was significantly greater than noise ($SNR > 2.82$).⁴¹

Figure 5A shows that the 31.25-Hz flicker ERG amplitude loss is associated with R_{mp3} loss, such that subjects with reduced 31.25 Hz flicker ERG amplitudes also have low R_{mp3} . Pearson correlation values are provided in each panel for the diabetic subjects ($n = 40$). There was no significant correlation between the 31.25-Hz amplitude loss and the log S loss (Fig. 5B). The combined cone a-wave parameters ($R_{mp3} + S$) were significantly correlated with the 31.25-Hz amplitude loss (Fig. 5C). Of note, the diabetic subjects generally had 31.25-Hz amplitudes that were within the range of the controls (one NDR and four mild NPDR subjects were below the lower limit of the control range). The bottom row of Figure 5 shows the relationships between the log 62.5-Hz amplitude loss and the three a-wave parameters. The strongest correlation was between the log 62.5-Hz amplitude loss and log $R_{mp3} + S$ loss (Fig. 5F). At 62.5 Hz, four NDR and six mild NPDR subjects had amplitudes that were below the lower limit of the control range. Thus, R_{mp3} is the best predictor of 31.25-Hz flicker ERG amplitude, whereas log $R_{mp3} + \log S$ is the best predictor of 62.5-Hz flicker ERG amplitude. As discussed below, this is expected based on the hypothesis that an R_{mp3} loss shifts the flicker function uniformly down (equally affecting the 31.25-Hz and 62.5-Hz amplitudes), whereas an S loss reduces the high-frequency amplitude (e.g., 62.5 Hz) more than middle- (e.g., 31.25 Hz) or low-frequency amplitudes.

Given the strong relationship between the a-wave parameters and the flicker ERG, it should be possible to generate the a-wave model fits for the patient groups based on their flicker ERG data. That is, the magnitude of 31.2-Hz flicker amplitude loss should correspond to the magnitude of the R_{mp3} loss; the magnitude of 62.5-Hz flicker amplitude loss should correspond to the magnitude of the log $R_{mp3} + \log S$ loss. This prediction

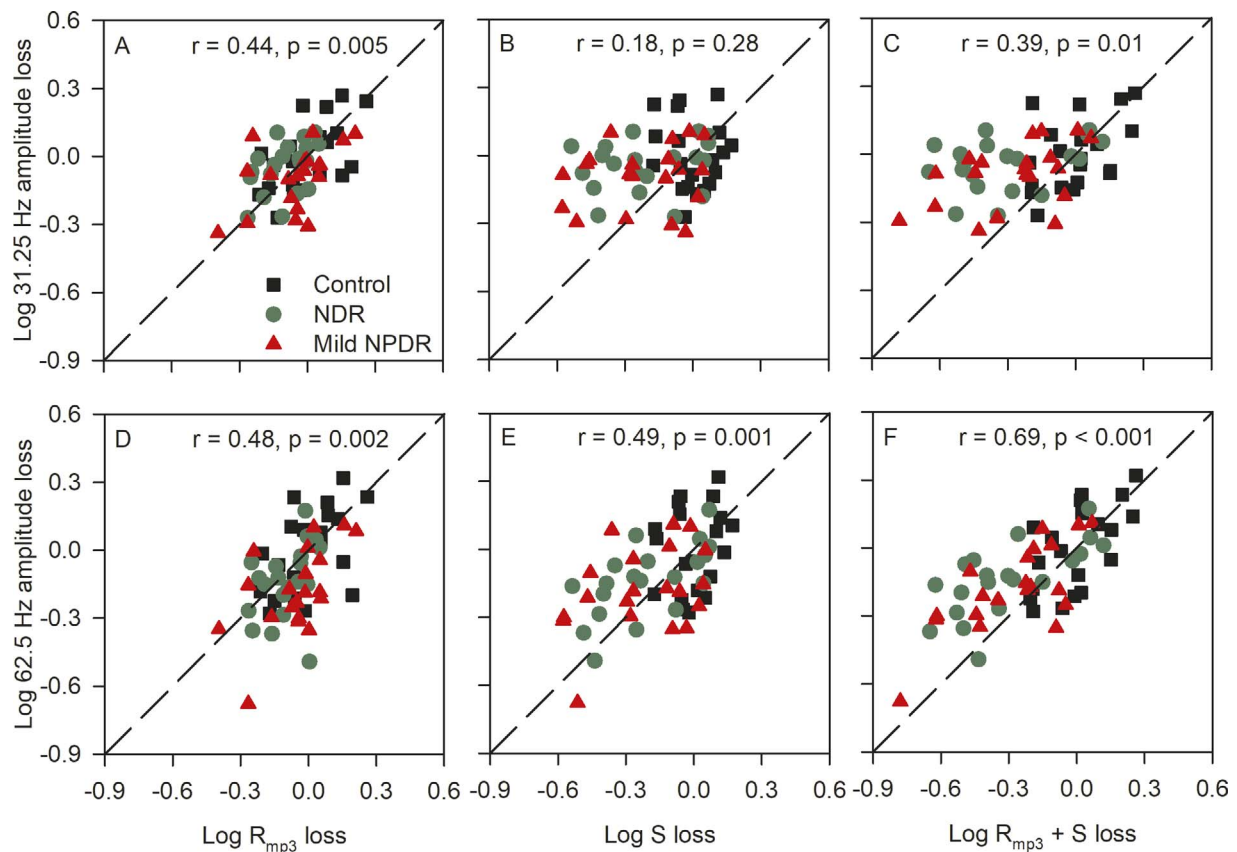


FIGURE 5. The relationship between the 31.25-Hz flicker ERG amplitude loss and the a-wave parameters is shown in the *top row* (A–C); the relationship between the 62.5-Hz flicker ERG amplitude loss and the a-wave parameters is shown in the *bottom row* (D–F). All measurements have been normalized to the control mean, as discussed in the text. The *dashed lines* have unit slope and mark equivalent losses for both parameters. Control subjects are shown in *black (squares)*, NDR subjects are shown in *green (circles)*, mild NPDR subjects are shown in *red (triangles)*. Pearson correlation values are provided in each panel for the combined diabetic groups ($n = 40$).

was examined as follows: first, the control, NDR, and mild NPDR a-waves for each flash retinal illuminance were replotted from Figure 1 in Figure 6 (solid lines). The control model fits were also replotted from Figure 1 (black dashed lines in Fig. 6). Next, the control model fit parameters (R_{mp3} and S) were adjusted based on the patients' relative attenuation of the 31.25-Hz and 62.5-Hz flicker responses. Specifically, for the NDR model prediction, $\log R_{mp3}$ was reduced from the control value of 1.72 to 1.68, because the 31.25-Hz flicker ERG was reduced by 0.04 log units for this group. Likewise, $\log S$ for the NDR group was reduced from 1.52 to 1.38, because the 62.5 Hz flicker response was reduced by 0.14 log units for this group. These parameters were entered into the model and the fit was generated for the four flash intensities, with the results shown in Figure 6 (green dashed lines). The same procedure was used to predict the fits for the mild NPDR group, with $\log R_{mp3}$ set to 1.63 and $\log S$ set to 1.34, given the relative flicker ERG losses at 31.25 Hz and 62.5 Hz for this group. The results of these predictions are shown as red dashed lines in Figure 6. The predicted model fits provided an excellent account of the waveforms for the diabetic groups. The root mean square (RMS) error between the data and the predicted model fit was 13.54 for the NDR group and 10.62 for the mild NPDR group (averaged over the four flash intensities). This compares favorably with the RMS error obtained when $\log R_{mp3}$ and $\log S$ were permitted to vary in the original calculations (i.e., Fig. 1; RMS error of 9.87 for the NDR group and 11.05 for the mild NPDR group).

Relationship Among OPs, Cone Phototransduction Parameters, and Flicker ERG Amplitude

As noted in the introduction, the OPs are commonly reported to be abnormal in DR. The relationship among these responses, the cone a-wave parameters, and the flicker ERG amplitudes was evaluated. The OPs were extracted from the 2.8 log Td-s single-flash response using conventional bandpass filtering techniques (70 Hz to 300 Hz).⁴² The trough-to-peak amplitude of the resulting four OPs was calculated and summed, according to convention.⁴⁵ ANOVA indicated that the OP log amplitude differed significantly among the three subject groups ($F = 4.28$, $P = 0.02$). Holm-Sidak pairwise comparisons indicated a statistically significant reduction in mean OP log amplitude for the NDR ($t = 2.53$, $P = 0.03$) and mild NPDR ($t = 2.54$, $P = 0.04$) groups compared with the controls. For the DR groups, OP log amplitude was significantly correlated with $\log S$ ($r = 0.40$, $P = 0.01$; $n = 40$), but not $\log R_{mp3}$ ($r = 0.01$, $P = 0.95$; $n = 40$). Likewise, OP log amplitude was not significantly correlated with either 31.25-Hz or 62.5-Hz flicker ERG log amplitude (both $r < 0.22$, $P > 0.17$). Thus, there were small, marginally significant, OP amplitude losses that were correlated with cone photoreceptor sensitivity.

DISCUSSION

The purpose of the present study was to develop a more complete understanding of the nature and extent of cone

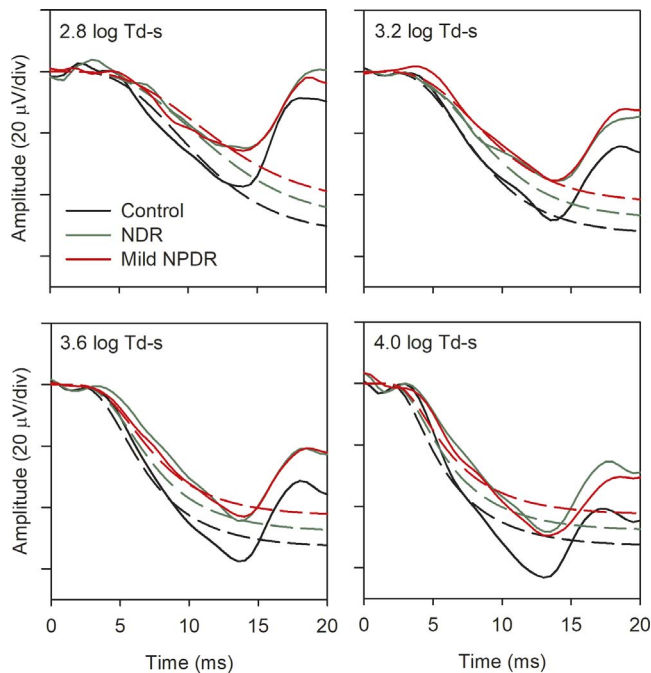


FIGURE 6. Mean single-flash ERG waveforms for each subject group are replotted from Figure 1 (controls, *black*; NDR, *green*; mild NPDR, *red*). Each panel shows data from a different flash retinal illuminance, as indicated in the figure. The *dashed lines* represent the delayed Gaussian model fits to the traces of the corresponding color that were generated based on the magnitude of $\log R_{mp3}$ and $\log S$ loss, as discussed in the text.

photoreceptor abnormalities in diabetic individuals who have NDR or mild NPDR. Specifically, we determined the extent to which abnormalities in the activation phase of cone phototransduction had predictable effects on the flicker ERG for individuals who have early-stage DR. Diabetes appears to have larger effects on cone photoreceptor sensitivity ($\log S$) than on the maximum a-wave amplitude ($\log R_{mp3}$). That is, 50% of the DM subjects had a $\log S$ value that was outside of the control range, whereas only 13% had a $\log R_{mp3}$ value that was outside of the control range; when present, the reductions in R_{mp3} were typically small (less than a factor of 1.14, on average). It was uncommon in our sample to find DM subjects who had reductions in both parameters (8% of the present sample). These findings are in accordance with previous work that showed that $\log S$ reductions were more frequently observed than $\log R_{mp3}$ reductions in diabetic individuals.²² In comparison with previous work, the present study included a larger sample of subjects that was restricted to diabetic individuals who had mild or no retinopathy. Nevertheless, the work of Holopigian et al.²² and the present study indicate that cone sensitivity losses in diabetic individuals are relatively common.

Based on the photoreceptor model of Lamb and Pugh⁴⁴ from which Hood and Birch's delayed Gaussian model²⁶ was derived, reductions in the sensitivity parameter ($\log S$) can be attributed to several factors. For example, alterations in quantal absorption that result from abnormalities within the phototransduction process could reduce $\log S$. Retinal hypoxia due to altered blood flow in the diabetic retina could also affect photoreceptor function, as suggested by Holopigian et al.²² Similarly, previous work has shown that central retinal vein occlusions reduce rod photoreceptor gain ($\log S$), with little effect on the a-wave maximum amplitude (R_{mp3}).⁴⁵ Thus, retinal hypoxia due to altered blood flow provides an attractive explanation for our results. However, a number of other

mechanisms can reduce $\log S$, including local morphological abnormalities of cone outer segments, decreased cone mitochondrial activity, and downregulation of cone protein expression,^{31,32} which the present findings cannot rule out.

In addition to abnormalities in the activation phase of cone phototransduction, the diabetic subjects also had amplitude losses of the high-frequency flicker ERG. The high-frequency attenuation became progressively greater as stimulus temporal frequency increased. For example, 12.5% of the diabetic subjects had 31.25-Hz flicker ERG amplitudes that were below the lower limit of the controls, 25% had reductions at 62.5 Hz, and 55% had reductions at 100 Hz. These high-frequency amplitude abnormalities were related to parameters derived from the activation phase of cone phototransduction discussed above. Specifically, the sum of the $\log R_{mp3}$ and $\log S$ parameters could be used to predict the patients' high-frequency (62.5 Hz) flicker ERG amplitude attenuation ($r = 0.69$, $P < 0.001$). $\log R_{mp3}$ alone was a reasonably good predictor of the small 31.25-Hz amplitude losses ($r = 0.44$, $P = 0.005$) and including $\log S$ in the correlation did not improve the correlation with the 31.25 Hz flicker ERG amplitude ($r = 0.39$, $P = 0.01$). These findings support previous work³¹ showing that the activation phase of cone phototransduction may be a major determinant of the high-frequency flicker ERG amplitude. Although the high-frequency flicker ERG is not likely a direct measure of cone photoreceptor function, the cones provide the initial input into the flicker ERG generators (i.e., ON and OFF bipolar cells^{46,47}). Thus, abnormal cone phototransduction is expected to have an impact on the characteristics of the high-frequency flicker ERG.

Although the fundamental amplitude of the high-frequency flicker ERG can be abnormal in early-stage DR, previous work has shown that the high-frequency harmonic response components elicited by slow flicker are generally normal.²⁸ For example, the mean fundamental response elicited by 62.5-Hz flicker was previously shown to be reduced significantly for diabetic subjects, but their fourth harmonic response to 16-Hz flicker (equivalent to 64 Hz) was not.²⁸ This finding was interpreted within the context of a linear-nonlinear-linear cascade model of retinal processing.^{29,30} This model posits a retinal nonlinearity that is "sandwiched" between two linear filters. As discussed in detail elsewhere,^{29,30} changes in the properties of the first linear filter, which is thought to be localized to the photoreceptors, could attenuate the fundamental response at high temporal frequencies without affecting the high-frequency harmonics elicited by slow flicker. This is because the harmonics are generated after the initial linear filter. Thus, previous findings based on modeling the flicker ERG also point to a photoreceptor source of the high-frequency attenuation, and are consistent with the reduced $\log S$ observed in the present study.

In addition to $\log S$ and the high-frequency flicker ERG amplitude reductions, OP amplitudes were also significantly reduced in both diabetic groups. Although the source of the OPs has not been established fully, there is general agreement that the later OPs are primarily generated by inner-retina neurons.⁴⁸⁻⁵⁰ In the present study, the amplitudes of the four OPs were derived and summed, an approach that has previously shown OP amplitude reductions in DR.^{20,51} Consistent with these previous studies, the OP amplitude was slightly, but significantly, reduced for both diabetic groups compared with the controls. Interestingly, $\log OP$ amplitude was correlated significantly with the $\log S$ parameter, suggesting that the OP amplitude reduction (presumed inner-retina dysfunction) may be secondary to photoreceptor changes. Alternatively, diabetes may independently affect both the OPs and cone phototransduction sensitivity. OP amplitude was not correlated significantly with the high-frequency flicker

ERG amplitude (62.5 Hz); however, it is possible that a stronger relationship between OP amplitude and flicker ERG amplitude could emerge if other definitions of the OPs were used. For example, future work could compare the amplitude of individual OPs to the flicker ERG amplitude, or examine the OPs elicited by different flash retinal illuminances (OPs in this study were derived from a flash luminance that was more than four times higher than the ISCEV standard 3.0 cd-s/m²). Previous studies have also shown value in quantifying OPs in the frequency spectrum^{52,53} and in the time-frequency spectrum.⁵⁴

In summary, most of the diabetic subjects in the present study had abnormalities in the activation phase of cone phototransduction (reduced log *S* and/or log *R_{mp3}*), with reduced log *S* being most commonly observed. The sum of these parameters was significantly correlated with the patients' flicker ERG amplitude losses at high temporal frequencies. These results indicate that the standard delayed Gaussian model of the a-wave is useful for characterizing abnormalities in the activation phase of cone phototransduction in diabetic individuals and has predictive value in accounting for flicker ERG abnormalities as well. Although DR is typically considered a disease of the retinal vasculature, the present results are consistent with evidence that diabetes can affect photoreceptor function.²⁴ Thus, there is a need for further studies of the role of photoreceptors in the pathogenesis of DR and the approach used in this study may be of use in this line of work.

Acknowledgments

Supported by National Institutes of Health research Grants R01EY026004 (JJM), P30EY001792 (core grant), an unrestricted departmental grant, and a Dolly Green Scholar award (JJM) from Research to Prevent Blindness.

Disclosure: **J.J. McAnany**, None; **J.C. Park**, None

References

- Barber AJ. A new view of diabetic retinopathy: a neurodegenerative disease of the eye. *Prog Neuropsychopharmacol Biol Psychiatry*. 2003;27:283–290.
- Barber AJ, Baccouche B. Neurodegeneration in diabetic retinopathy: potential for novel therapies. *Vision Res*. 2017;139:82–92.
- Lieth E, Gardner TW, Barber AJ, Antonetti DA; Penn State Retina Research Group. Retinal neurodegeneration: early pathology in diabetes. *Clin Exp Ophthalmol*. 2000;28:3–8.
- Lynch SK, Abramoff MD. Diabetic retinopathy is a neurodegenerative disorder. *Vision Res*. 2017;139:101–107.
- Sohn EH, van Dijk HW, Jiao C, et al. Retinal neurodegeneration may precede microvascular changes characteristic of diabetic retinopathy in diabetes mellitus. *Proc Natl Acad Sci U S A*. 2016;113:E2655–E2664.
- van Dijk HW, Kok PH, Garvin M, et al. Selective loss of inner retinal layer thickness in type 1 diabetic patients with minimal diabetic retinopathy. *Invest Ophthalmol Vis Sci*. 2009;50:3404–3409.
- van Dijk HW, Verbraak FD, Kok PH, et al. Decreased retinal ganglion cell layer thickness in patients with type 1 diabetes. *Invest Ophthalmol Vis Sci*. 2010;51:3660–3665.
- van Dijk HW, Verbraak FD, Kok PH, et al. Early neurodegeneration in the retina of type 2 diabetic patients. *Invest Ophthalmol Vis Sci*. 2012;53:2715–2719.
- van Dijk HW, Verbraak FD, Stehouwer M, et al. Association of visual function and ganglion cell layer thickness in patients with diabetes mellitus type 1 and no or minimal diabetic retinopathy. *Vision Res*. 2011;51:224–228.
- Arden GB, Hamilton AM, Wilson-Holt J, Ryan S, Yudkin JS, Kurtz A. Pattern electroretinograms become abnormal when background diabetic retinopathy deteriorates to a preproliferative stage: possible use as a screening test. *Br J Ophthalmol*. 1986;70:330–335.
- Boschi MC, Frosini R, Mencucci R, Sodi A. The influence of early diabetes on the pattern electroretinogram. *Doc Ophthalmol*. 1989;71:369–374.
- Caputo S, Di Leo MA, Falsini B, et al. Evidence for early impairment of macular function with pattern ERG in type 1 diabetic patients. *Diabetes Care*. 1990;13:412–418.
- Coupland SG. A comparison of oscillatory potential and pattern electroretinogram measures in diabetic retinopathy. *Doc Ophthalmol*. 1987;66:207–218.
- Prager TC, Garcia CA, Mincher CA, Mishra J, Chu HH. The pattern electroretinogram in diabetes. *Am J Ophthalmol*. 1990;109:279–284.
- Chen H, Zhang M, Huang S, Wu D. The photopic negative response of flash ERG in nonproliferative diabetic retinopathy. *Doc Ophthalmol*. 2008;117:129–135.
- Kizawa J, Machida S, Kobayashi T, Gotoh Y, Kurosaka D. Changes of oscillatory potentials and photopic negative response in patients with early diabetic retinopathy. *Jpn J Ophthalmol*. 2006;50:367–373.
- Aylward GW. The scotopic threshold response in diabetic retinopathy. *Eye (Lond)*. 1989;3(Pt 5):626–637.
- Feigl B, Zele AJ, Fader SM, et al. The post-illumination pupil response of melanopsin-expressing intrinsically photosensitive retinal ganglion cells in diabetes. *Acta Ophthalmol*. 2012;90:e230–e234.
- Park JC, Chen YF, Blair NP, et al. Pupillary responses in nonproliferative diabetic retinopathy. *Sci Rep*. 2017;7:44987.
- Tzekov R, Arden GB. The electroretinogram in diabetic retinopathy. *Surv Ophthalmol*. 1999;44:53–60.
- Elsner AE, Burns SA, Lobes LA Jr, Doft BH. Cone photopigment bleaching abnormalities in diabetes. *Invest Ophthalmol Vis Sci*. 1987;28:718–724.
- Holopigian K, Greenstein VC, Seiple W, Hood DC, Carr RE. Evidence for photoreceptor changes in patients with diabetic retinopathy. *Invest Ophthalmol Vis Sci*. 1997;38:2355–2365.
- Kern TS. Do photoreceptor cells cause the development of retinal vascular disease? *Vision Res*. 2017;139:65–71.
- Kern TS, Berkowitz BA. Photoreceptors in diabetic retinopathy. *J Diabetes Investig*. 2015;6:371–380.
- Hood DC, Birch DG. Rod phototransduction in retinitis pigmentosa: estimation and interpretation of parameters derived from the rod a-wave. *Invest Ophthalmol Vis Sci*. 1994;35:2948–2961.
- Hood DC, Birch DG. Phototransduction in human cones measured using the alpha-wave of the ERG. *Vision Res*. 1995;35:2801–2810.
- McAnany JJ, Park JC, Chau FY, et al. Amplitude loss of the high-frequency flicker electroretinogram in early diabetic retinopathy [published online ahead of print July 16, 2018]. *Retina*. doi:10.1097/IAE.0000000000002262.
- McAnany JJ, Park JC. Temporal frequency abnormalities in early-stage diabetic retinopathy assessed by electroretinography. *Invest Ophthalmol Vis Sci*. 2018;59:4871–4879.
- Alexander KR, Fishman GA, Grover S. Temporal frequency deficits in the electroretinogram of the cone system in X-linked retinoschisis. *Vision Res*. 2000;40:2861–2868.
- Burns SA, Elsner AE, Kreitz MR. Analysis of nonlinearities in the flicker ERG. *Optom Vis Sci*. 1992;69:95–105.
- Alexander KR, Rajagopalan AS, Raghuram A, Fishman GA. Activation phase of cone phototransduction and the flicker

- electroretinogram in retinitis pigmentosa. *Vision Res.* 2006; 46:2773-2785.
32. Tzekov RT, Locke KG, Hood DC, Birch DG. Cone and rod ERG phototransduction parameters in retinitis pigmentosa. *Invest Ophthalmol Vis Sci.* 2003;44:3993-4000.
 33. Hood DC, Birch DG. Assessing abnormal rod photoreceptor activity with the a-wave of the electroretinogram: applications and methods. *Doc Ophthalmol.* 1996;92:253-267.
 34. Wu S, Burns SA. Analysis of retinal light adaptation with the flicker electroretinogram. *J Opt Soc Am A Opt Image Sci Vis.* 1996;13:649-657.
 35. Davis MD, Fisher MR, Gangnon RE, et al. Risk factors for high-risk proliferative diabetic retinopathy and severe visual loss: Early Treatment Diabetic Retinopathy Study Report #18. *Invest Ophthalmol Vis Sci.* 1998;39:233-252.
 36. Park JC, Cao D, Collison FT, Fishman GA, McAnany JJ. Rod and cone contributions to the dark-adapted 15-Hz flicker electroretinogram. *Doc Ophthalmol.* 2015;130:111-119.
 37. Friedburg C, Allen CP, Mason PJ, Lamb TD. Contribution of cone photoreceptors and post-receptor mechanisms to the human photopic electroretinogram. *J Physiol.* 2004;556:819-834.
 38. Ueno S, Kondo M, Niwa Y, Terasaki H, Miyake Y. Luminance dependence of neural components that underlies the primate photopic electroretinogram. *Invest Ophthalmol Vis Sci.* 2004; 45:1033-1040.
 39. Robson JG, Saszik SM, Ahmed J, Frishman LJ. Rod and cone contributions to the a-wave of the electroretinogram of the macaque. *J Physiol.* 2003;547:509-530.
 40. Bush RA, Sieving PA. A proximal retinal component in the primate photopic ERG a-wave. *Invest Ophthalmol Vis Sci.* 1994;35:635-645.
 41. Meigen T, Bach M. On the statistical significance of electrophysiological steady-state responses. *Doc Ophthalmol.* 1999;98:207-232.
 42. Khani-Oskouee K, Sieving PA. A digital band-pass filter for electrophysiology recording systems. In: Heckenlively J, Arden G, eds. *Principles and Practice of Clinical Electrophysiology of Vision.* St. Louis, MO: Mosby Year Book; 1991: 205-210.
 43. Bresnick GH, Korth K, Groo A, Palta M. Electroretinographic oscillatory potentials predict progression of diabetic retinopathy. Preliminary report. *Arch Ophthalmol.* 1984;102:1307-1311.
 44. Lamb TD, Pugh EN Jr. A quantitative account of the activation steps involved in phototransduction in amphibian photoreceptors. *J Physiol.* 1992;449:719-758.
 45. Shady S, Hood DC, Birch DG. Rod phototransduction in retinitis pigmentosa. Distinguishing alternative mechanisms of degeneration. *Invest Ophthalmol Vis Sci.* 1995;36:1027-1037.
 46. Kondo M, Sieving PA. Primate photopic sine-wave flicker ERG: vector modeling analysis of component origins using glutamate analogs. *Invest Ophthalmol Vis Sci.* 2001;42:305-312.
 47. Kondo M, Sieving PA. Post-photoreceptor activity dominates primate photopic 32-Hz ERG for sine-, square-, and pulsed stimuli. *Invest Ophthalmol Vis Sci.* 2002;43:2500-2507.
 48. Dai J, He J, Wang G, Wang M, Li S, Yin ZQ. Contribution of GABA_A, GABA_C and glycine receptors to rat dark-adapted oscillatory potentials in the time and frequency domain. *Oncotarget.* 2017;8:77696-77709.
 49. Wachtmeister L, Dowling JE. The oscillatory potentials of the mudpuppy retina. *Invest Ophthalmol Vis Sci.* 1978;17:1176-1188.
 50. Ogden TE. The oscillatory waves of the primate electroretinogram. *Vision Res.* 1973;13:1059-1074.
 51. Bresnick GH, Palta M. Oscillatory potential amplitudes. Relation to severity of diabetic retinopathy. *Arch Ophthalmol.* 1987;105:929-933.
 52. Li XX, Yuan N. Measurement of the oscillatory potential of the electroretinogram in the domains of frequency and time. *Doc Ophthalmol.* 1990;76:65-71.
 53. Van der Torren K, Groeneweg G, van Lith G. Measuring oscillatory potentials: Fourier analysis. *Doc Ophthalmol.* 1988;69:153-159.
 54. Gauvin M, Dorfman AL, Trang N, et al. Assessing the contribution of the oscillatory potentials to the genesis of the photopic ERG with the discrete wavelet transform. *Biomed Res Int.* 2016;2016:2790194.